Available online at www.sciencedirect.com
SCIENCE DIRECT®
Optics Communications 254 (2005) 152–167
OPTICS COMMUNICATIONS
www.elsevier.com/locate/optcom

Theoretical investigation of the NOLM with highly twisted fibre and a $\lambda/4$ birefringence bias

O. Pottiez [a,*], E.A. Kuzin [b], B. Ibarra-Escamilla [b], F. Méndez-Martínez [a]

[a] *Postdoctoral Researcher of FNRS (Belgian Fund for Scientific Research), Service d'Electromagnétisme et de Télécommunications, Faculté Polytechnique de Mons, Boulevard Dolez 31, B-7000 Mons, Belgium*
[b] *Instituto Nacional de Astrofísica, Óptica y Electrónica (INAOE), L. E. Erro 1, Tonantzintla, 72000 Puebla, Pue., Mexico*

Received 3 March 2005; accepted 11 May 2005

Abstract

We investigate theoretically the operation of a novel, power-symmetric nonlinear optical loop mirror (NOLM) scheme, which relies on nonlinear polarisation rotation. The device is made of a symmetrical coupler, highly twisted fibre and a quarter wave plate (QWP) located asymmetrically in the loop, which can be rotated in a plane perpendicular to the fibre. Using a weak nonlinearity approach, the nonlinear NOLM transmission is accurately determined through a simple matrix description. For substantial twist, a simple though general analytical expression of the NOLM power transmission is found. This transmission strongly depends on the QWP angle, but also on the polarisation state at the NOLM input. This analysis allows to infer interesting properties of the switching characteristic, in particular its flexibility and, in some cases, its stability against small changes of input polarisation. The QWP angle and the input polarisation state are the control parameters through which the transmission can be adjusted in a versatile way, making the device attractive for various applications. Although the polarisation obtained at the NOLM output is power-dependent in general, we show that, for particular configurations, the output polarisation is constant with power. This is particularly interesting in the frame of polarisation-sensitive applications. We believe that the proposed model will be very useful to optimise the design and control of the proposed NOLM structure, which has the potential to play an important role in future ultrafast optical communication systems.

PACS: 07.60.Vg; 42.65.Pc; 42.81.Gs

Keywords: Sagnac interferometer; Fibre-optic devices; Optical communications

* Corresponding author. Tel.: +32 65 37 41 48; fax: +32 65 37 41 99.
E-mail address: pottiez@telecom.fpms.ac.be (O. Pottiez).

0030-4018/$ - see front matter © 2005 Elsevier B.V. All rights reserved.
doi:10.1016/j.optcom.2005.05.015

1. Introduction

The fibre nonlinear Sagnac interferometer, or nonlinear optical loop mirror (NOLM) [1], is commonly used today in many applications, including optical switching and demultiplexing [2], all-optical active mode locking [3], passive mode locking [4], pedestal suppression [5], pulse shaping or regeneration of ultrafast data streams [6]. This simple device, made of a coupler whose output ports are connected through a span of fibre, offers a versatile way to obtain a nonlinear transmission (or switching) characteristic through the optical Kerr effect, if a nonlinear phase shift difference appears between the two interfering beams. When a polarisation controller is inserted in the loop, the bias of the switching characteristic can be adjusted to meet the requirements of a specific application. Most NOLM designs rely on self-phase modulation, which allows a differential nonlinear phase shift to accumulate only if a power imbalance exists between the beams propagating clockwise (CW) and counterclockwise (CCW) in the loop. As the power ratio between CW and CCW beams is generally imposed by construction (in general, through the fixed coupling ratio of the coupler), such designs offer few possibilities of adjustment, especially in terms of contrast or critical power (power difference between minimal and maximal transmissions, corresponding to a π nonlinear phase shift difference). In addition, when designing such a NOLM, a compromise often has to be found between high contrast, low critical power and low insertion loss, as in general the three criteria cannot be met simultaneously.

A change occurred when it was realized that, thanks to the nonlinear polarisation rotation (NPR) phenomenon, a polarisation asymmetry between the CW and CCW beams can provide switching, even if powers are equal (case of a symmetrical coupler) [7,8]. A particularly promising NOLM structure, made of a symmetrical coupler, highly twisted fibre and a quarter wave plate (QWP), and operating through NPR was proposed in [8]. In a previous publication, we studied theoretically the operation of this NOLM in the weakly nonlinear regime, in the particular case of circular input polarisation [9]. In this paper, we propose a complete theoretical description of the NOLM operation in the weakly nonlinear regime, which accounts for all possible input polarisation states.

A rather clear picture of the operation of a NOLM can be obtained by considering the coupled equations for nonlinear polarisation evolution in the continuous-wave case [10], which describe the propagation of a polarised beam of power P down a fibre span:

$$\begin{aligned}\partial_z C^+ &= \mathrm{i}bP\left(|C^+|^2 + 2|C^-|^2\right)C^+ = \mathrm{i}bP\left(\frac{3}{2} - \frac{1}{2}A_s\right)C^+;\\ \partial_z C^- &= \mathrm{i}bP\left(|C^-|^2 + 2|C^+|^2\right)C^- = \mathrm{i}bP\left(\frac{3}{2} + \frac{1}{2}A_s\right)C^+.\end{aligned} \tag{1}$$

In Eq. (1), ∂_z denotes the first derivative with respect to the direction of propagation z, $b = 4\pi\tilde{n}_2/3\lambda A_{\mathrm{eff}}$ is the nonlinearity coefficient ($\tilde{n}_2$ being the Kerr coefficient, λ the wavelength and A_{eff} the effective modal area), and C^+ and C^- are the complex amplitudes of the circular right and left polarization components, respectively, normalized to the power P, in such a way that $|C^+|^2 + |C^-|^2 = 1$. Finally, $A_s = |C^+|^2 - |C^-|^2$ is the Stokes parameter. In the right-hand sides of Eq. (1), we omitted the linear terms, which account for linear birefringence and optical activity (circular birefringence). These equations show that propagation down the fibre has two consequences on the beam properties, causing per unit length a phase shift = $3/2bP$, and an ellipse rotation = $-1/2A_sbP$ (note that, to simplify the discussion, we make this distinction formally even for circular polarisation ($A_s = \pm 1$), yet in that case a phase shift and a rotation have the same effect on the polarisation). If Eq. (1) is applied to each of the two beams that counterpropagate in a NOLM structure, it appears clearly that the nonlinear phase shifts between CW and CCW beams will be different only if their powers are different. This is the main outcome of the conventional NOLM model [1]. In contrast, a difference of NPR can exist for equal

powers, provided that the Stokes parameters (the polarisation states) are different. When the beams recombine at the NOLM output, a differential NPR is responsible for a power-dependent transmission characteristic, similarly to a differential nonlinear phase shift. However, whereas a power imbalance can be easily maintained during propagation, allowing the nonlinear phase shift difference to accumulate, an initial difference of polarisation states tends to be lost rapidly in practice, causing the differential NPR to vanish, because of changes of polarisation due to residual birefringence, which is unavoidable in a standard fibre. In order to obtain NPR-based switching, care has thus to be taken that the polarisation ellipses be conserved during propagation.

2. Modelling

The structure under study is shown in Fig. 1. It consists of a 50/50 coupler, a span of low-linear-birefringence, highly twisted fibre connecting the two output ports of the coupler, and a QWP inserted in the loop, close to the coupler. In such power-symmetric design, different nonlinear evolutions can only be obtained through the polarisation difference generated by the QWP. The QWP can be rotated in a plane perpendicular to the fibre, its angle α is defined as shown in Fig. 1. The purpose of the strong twist applied to the fibre is to overcome its residual (intrinsic and stress-induced) birefringence, which also depends on environmental conditions. Indeed, this twist generates high optical activity (circular birefringence) along the fibre, and also causes a rapid precession of its principal axes. Both effects tend to conserve the polarisation ellipticity of each of the counterpropagating beams during propagation in the loop. This allows NPR difference to build up, and generate switching. Twist also makes the interferometer more robust against environmental perturbations.

In most cases, although the general coupled equations in the continuous wave case (Eqs. (1) including birefringence terms) can be solved analytically in terms of elliptic functions [10], such solutions are of limited utility for our purpose. These equations can be used however to derive a set of approximate equations, which are valid in the weak-nonlinearity regime [8]. These two differential equations are expressed in the basis of the polarisation eigenmodes, which are generally elliptical, [S^+, S^-]. These equations can be written as:

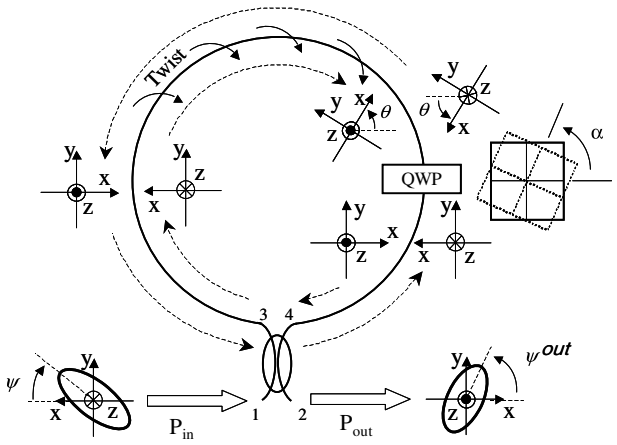

Fig. 1. Scheme of the NOLM structure investigated in this paper, including the coordinate frames used. These frames twist along with the fibre (in a plane perpendicular to its axis). Note the $-\theta$ rotation of the frames through the QWP. Frames of CW and CCW beams only coincide at the NOLM input and output.

$$\begin{aligned} \mathrm{i}\partial_s S^+ &= \left[-\mu - \frac{1}{2}(3 - A_S)P_N\right]S^+; \\ \mathrm{i}\partial_s S^- &= \left[+\mu - \frac{1}{2}(3 + A_S)P_N\right]S^-, \end{aligned} \tag{2}$$

where $A_s = |S^+|^2 - |S^-|^2$ is constant during propagation. In the case of high twist, eigenmodes coincide approximately with circular polarisation states [C^+, C^-]. The basis employed here is rotating, as it twists along with the fibre, at a rate corresponding to the twist rate, q. In Eqs. (2), $\mu = \sqrt{(\pi^2 + g^2)}$, where $g = \gamma\pi/k$ is the ratio of circular to linear birefringence, $k = \pi\delta n/\lambda$ describing the linear birefringence, and $\gamma = [h/(2n) - 1]q$ the circular birefringence, in the rotating frame (n is the refractive index and $h \approx 0.13$–0.16 in silica fibre). $P_N = b\pi P/k$ is the normalised power, where P is the power into the fibre and $b = 4\pi\tilde{n}_2/3\lambda A_{\mathrm{eff}}$ is the nonlinearity coefficient. The derivatives are taken with respect to a normalized length $s = zk/\pi = z/L_b$, where z is the absolute length (in m) and L_b the fibre beat length. These simple equations can easily be integrated over the fibre length $l = L/L_b$. This in turn allows a matrix representation of the fibre span in the eigenmodes basis:

$$F_{\mathrm{cw/ccw}} = \begin{bmatrix} \mathrm{e}^{\mathrm{i}\left[\mu + \frac{1}{4}\left(3 - A_s^{\mathrm{cw/ccw}}\right)P_{\mathrm{in}}\right]l} & 0 \\ 0 & \mathrm{e}^{\mathrm{i}\left[-\mu + \frac{1}{4}\left(3 + A_s^{\mathrm{cw/ccw}}\right)P_{\mathrm{in}}\right]l} \end{bmatrix} = \begin{bmatrix} \mathrm{e}^{\mathrm{i}\left(\varphi + r_{\mathrm{cw/ccw}}\right)} & 0 \\ 0 & \mathrm{e}^{\mathrm{i}\left(\varphi - r_{\mathrm{cw/ccw}}\right)} \end{bmatrix}, \tag{3}$$

where $P_{\mathrm{in}} = 2P_N$ is the input power to the NOLM, and the superscripts cw and ccw apply for clockwise and counterclockwise beams, respectively. Eq. (3) again allows individualising two nonlinear effects: a nonlinear phase shift $\varphi = 3/4P_{\mathrm{in}}l$, and a polarisation-dependent rotation of the ellipse, $-1/4A_s^{\mathrm{cw/ccw}}P_{\mathrm{in}}l$, which adds to the linear rotation μl to yield $r_{\mathrm{cw/ccw}}$, the total rotation.

Once the nonlinearity in the fibre can be modelled by a matrix, the complete NOLM behaviour can be described using the same approach. Indeed, if each element in the system is represented by its transfer matrix, one can determine, using simple matrix algebra, the Jones vector at the NOLM output, and thus the value of transmission, for any given input power and polarisation state.

In the [C^+, C^-] basis, the transfer matrix of the QWP writes as, for the CW beam:

$$\mathrm{QWP}_{\mathrm{cw}} = \begin{bmatrix} \frac{1+\mathrm{i}}{2} & \frac{1-i}{2}\mathrm{e}^{2\mathrm{i}\alpha} \\ \frac{1-\mathrm{i}}{2}\mathrm{e}^{-2\mathrm{i}\alpha} & \frac{1+\mathrm{i}}{2} \end{bmatrix}, \tag{4}$$

The matrix for the CCW beam, $\mathrm{QWP}_{\mathrm{ccw}}$, is obtained by replacing α by $-\alpha$ in Eq. (4). Note that the QWP angle α is defined in a frame having its y-axis perpendicular to the plane of the loop, and not in the rotating frame (see Fig. 1). This change of frame between the fibre and the QWP (and conversely) is taken into account by the matrix:

$$\Theta = \begin{bmatrix} \mathrm{e}^{\mathrm{i}\theta} & 0 \\ 0 & \mathrm{e}^{-\mathrm{i}\theta} \end{bmatrix}, \tag{5}$$

where $\theta = qL$ is the total twist of the fibre. The Jones vector at the NOLM input can be expressed (in the circular basis) as $E_{\mathrm{in}} = [U\exp(\mathrm{i}\psi); V\exp(-\mathrm{i}\psi)]$, where U, V are real positive and obey $U^2 + V^2 = 1$. The polarisation state is completely determined by the Stokes parameter, $A_s^{\mathrm{in}} = U^2 - V^2$, which defines the shape of the ellipse (including the sense of polarisation, right or left), and the angle ψ, which defines the direction of the ellipse major axis in the chosen frame (see Fig. 1). Finally, it is assumed here that the coupler has no birefringence, so that in particular the Stokes parameter at the NOLM input $A_s^{\mathrm{in}} = A_s^{\mathrm{cw}}$.

It is now straightforward to calculate, for any input polarisation, the Jones vector of the output field. It is obtained by making the sum of the CW and CCW fields which interfere at the NOLM output. These are, respectively:

$$E_{\text{out}}^{\text{cw}} = \frac{1}{2}\text{QWP}_{\text{cw}} \times \Theta \times F_{\text{cw}} \times E_{\text{in}};$$
$$E_{\text{out}}^{\text{ccw}} = -\frac{1}{2}F_{\text{ccw}} \times \Theta \times \text{QWP}_{\text{ccw}} \times E_{\text{in}}. \tag{6}$$

The minus sign in the second part of Eq. (6) takes into account the two π/2 phase shifts undergone by the CCW beam at the coupler (crossing from port 1 to 4 and 3 to 2). Note that, in the following, it will be assumed that all matrixes involved in Eq. (6) are expressed in the $[C^+, C^-]$ basis. As the matrixes F_{cw} and F_{ccw} given by Eq. (3) are expressed in the eigenmodes basis, which corresponds to the circular basis only if twist is infinite, all the following developments will be correct, strictly speaking, only in this limit. Note however that, in itself, the matrix formulation given by Eq. (6) is valid (in the weak nonlinearity limit) for any value of twist, provided that a proper change of basis is applied to the matrixes F_{cw} and F_{ccw}.

After some calculation, the following expression is found for the output field:

$$E_{\text{out}} = E_{\text{out}}^{\text{cw}} + E_{\text{out}}^{\text{ccw}} = \begin{bmatrix} C_{\text{out}}^{+} \\ C_{\text{out}}^{-} \end{bmatrix}$$
$$= \begin{bmatrix} U\frac{\text{i}-1}{2}\sin\left(\frac{r_{\text{cw}}-r_{\text{ccw}}}{2}\right)\text{e}^{\text{i}\left(\varphi+\frac{r_{\text{cw}}+r_{\text{ccw}}}{2}+\psi+\theta\right)} + V\frac{\text{i}+1}{2}\sin\left(-\frac{r_{\text{cw}}+r_{\text{ccw}}}{2}+2\alpha-\theta\right)\text{e}^{\text{i}\left(\varphi+\frac{r_{\text{ccw}}-r_{\text{cw}}}{2}-\psi\right)} \\ U\frac{\text{i}+1}{2}\sin\left(\frac{r_{\text{cw}}+r_{\text{ccw}}}{2}-2\alpha+\theta\right)\text{e}^{\text{i}\left(\varphi+\frac{r_{\text{cw}}-r_{\text{ccw}}}{2}+\psi\right)} + V\frac{\text{i}-1}{2}\sin\left(\frac{r_{\text{ccw}}-r_{\text{cw}}}{2}\right)\text{e}^{\text{i}\left(\varphi-\frac{r_{\text{cw}}+r_{\text{ccw}}}{2}-\psi-\theta\right)} \end{bmatrix}. \tag{7}$$

From this result, expressions for the square modules of the two circular components of E_{out} can be found easily:

$$|C_{\text{out}}^{+}|^2 = \frac{U^2}{2}\sin^2\left(\frac{r_{\text{cw}}-r_{\text{ccw}}}{2}\right) + \frac{V^2}{2}\sin^2\left(-\frac{r_{\text{cw}}+r_{\text{ccw}}}{2}+2\alpha-\theta\right)$$
$$- UV\sin\left(\frac{r_{\text{cw}}-r_{\text{ccw}}}{2}\right)\sin\left(-\frac{r_{\text{cw}}+r_{\text{ccw}}}{2}+2\alpha-\theta\right)\sin\left(r_{\text{cw}}+2\psi+\theta\right);$$
$$|C_{\text{out}}^{-}|^2 = \frac{U^2}{2}\sin^2\left(\frac{r_{\text{cw}}+r_{\text{ccw}}}{2}-2\alpha+\theta\right) + \frac{V^2}{2}\sin^2\left(\frac{r_{\text{ccw}}-r_{\text{cw}}}{2}\right)$$
$$+ UV\sin\left(\frac{r_{\text{cw}}+r_{\text{ccw}}}{2}-2\alpha+\theta\right)\sin\left(\frac{r_{\text{ccw}}-r_{\text{cw}}}{2}\right)\sin\left(r_{\text{cw}}+2\psi+\theta\right). \tag{8}$$

Eqs. (8) then yield the following expression for the power transmission of the NOLM:

$$T = \frac{P_{\text{out}}}{P_{\text{in}}} = |C_{\text{out}}^{+}|^2 + |C_{\text{out}}^{-}|^2$$
$$= \frac{1}{2} - \frac{1}{4}\cos\left[\frac{1}{4}\left(A_{\text{s}}^{\text{cw}} - A_{\text{s}}^{\text{ccw}}\right)P_{\text{in}}l\right] - \frac{1}{4}\cos\left[2\mu l + 2\theta - 4\alpha - \frac{1}{4}\left(A_{\text{s}}^{\text{cw}} + A_{\text{s}}^{\text{ccw}}\right)P_{\text{in}}l\right]$$
$$= \frac{1}{2} - \frac{1}{2}\cos\left(\mu l + \theta - 2\alpha - \frac{1}{4}A_{\text{s}}^{\text{cw}}P_{\text{in}}l\right)\cos\left(\mu l + \theta - 2\alpha - \frac{1}{4}A_{\text{s}}^{\text{ccw}}P_{\text{in}}l\right). \tag{9}$$

Let us define $\beta = \mu l + \theta$. In the case of high twist, we have $\mu = \sqrt{(g^2 + \pi^2)} \approx g$, so that $\beta \approx gl + \theta = hqL/(2n) = \rho L$, where ρ is the rotatory power (in rad/m). Hence, in this limit, β can be interpreted as the total optical activity of the fibre. However, as the value of β is relevant only modulo 2π, the error resulting from this approximation, $\beta - \rho L = (\mu - g)l \approx \pi^2 l/(2g)$ can be substantial in practice (using the values $g = 100$ and $l = 10$, the mismatch amounts to about 8% of π). It is thus recommended to use the definition of β in calculations. Finally, the transmission writes as:

$$T = \frac{1}{2} - \frac{1}{2}\cos\left(\beta - 2\alpha - \frac{1}{4}A_{\text{s}}^{\text{cw}}P_{\text{in}}l\right)\cos\left(\beta - 2\alpha - \frac{1}{4}A_{\text{s}}^{\text{ccw}}P_{\text{in}}l\right), \tag{10}$$

where $A_s^{cw} = A_s^{in}$. Calculating $QWP_{ccw}E_{in}$, we can determine the value of A_s^{ccw}:

$$A_s^{ccw} = -\sqrt{1 - A_s^{cw2}}\sin 2(\alpha + \psi). \tag{11}$$

Again, it is assumed here that the coupler introduces no birefringence. Eqs. (10) and (11) constitute a very simple analytic expression of the NOLM transmission which is valid for any input polarisation (defined by A_s^{cw} and ψ) and power. This expression thus provides with a helpful tool to proceed to a detailed analysis of the NOLM behaviour in different conditions.

3. Study of the NOLM transmission for different input polarisations

3.1. Circular input polarisation

In the case of circular-right polarisation, $A_s^{cw} = 1$ $(U = 1,\ V = 0)$, and $A_s^{cw} = -1$ $(U = 0,\ V = 1)$ in the case of circular-left input polarisation. In both situations, Eq. (11) shows that $A_s^{ccw} = 0$ (the CCW beam is linearly polarised). Eq. (10) then becomes

$$T = \frac{1}{2} - \frac{1}{2}\cos(\beta - 2\alpha)\cos\left(\beta - 2\alpha \mp \frac{1}{4}P_{in}l\right), \tag{12}$$

where the sign of the nonlinear term is determined by the sense of circular polarisation. This case has already been investigated elsewhere [9,11]. The transmission is a sinusoidal function of P_{in}, whose contrast (ratio between maximum and minimum values) can be set to any value between 1 and ∞ through the adjustment of the QWP angle, α. Thanks to this possibility, high-order amplitude equalisation of an optical pulse train was recently demonstrated using this setup [12]. Note that α also determines the phase of the nonlinear transmission characteristic, and allows to adjust low-power transmission between 0 and 0.5. In contrast, the critical power (defined here as the power at which NPR difference reaches π), $P_\pi = 4\pi/l$, does not depend on α. An optimal, infinite-contrast switching characteristic (minimal transmission = 0 at low power, maximal transmission = 1 at $P_{in} = P_\pi$) is obtained for $\alpha = \beta/2 + k\pi/2$, k integer.

Fig. 2(a) presents the curves given by Eq. (12) for different values of α. For comparison, the figure also shows the transmission curves obtained through numerical integration of the general coupled equations, taking $g = 100$ and $l = 10$. For a beat length $L_b \approx 15$ m (which was measured for SMF-28 fibre [13]), this value of g corresponds to a twist rate of about 1 turn/m, which is rather small in practice (values of 6–7 turns/m were used in previous experiments). The figure shows that the curves obtained analytically and numerically agree quite well in general. Some differences are observed however, which are mainly due to the approximation of taking circular polarisation modes as the eigenmodes (approximation of infinite twist). In contrast, the discrepancies originating from the weak nonlinearity approximation [8] were shown to be very small in the range of power considered. The differences observed in Fig. 2(a) thus vanish for higher values of twist.

3.2. Linear input polarisation

We have in this case $A_s^{cw} = 0$ $(U = V = \sqrt{2}/2)$, and Eqs. (10) and (11) lead to

$$T = \frac{1}{2} - \frac{1}{2}\cos(\beta - 2\alpha)\cos\left\{\beta - 2\alpha + \frac{1}{4}P_{in}l\sin[2(\alpha + \psi)]\right\}. \tag{13}$$

It is noticeable here that the critical power, $P_\pi = 4\pi/|l\sin 2(\alpha + \psi)|$ depends on both α and the polarisation direction ψ, so that it can be adjusted by tuning any of these two parameters. An easily adjustable critical

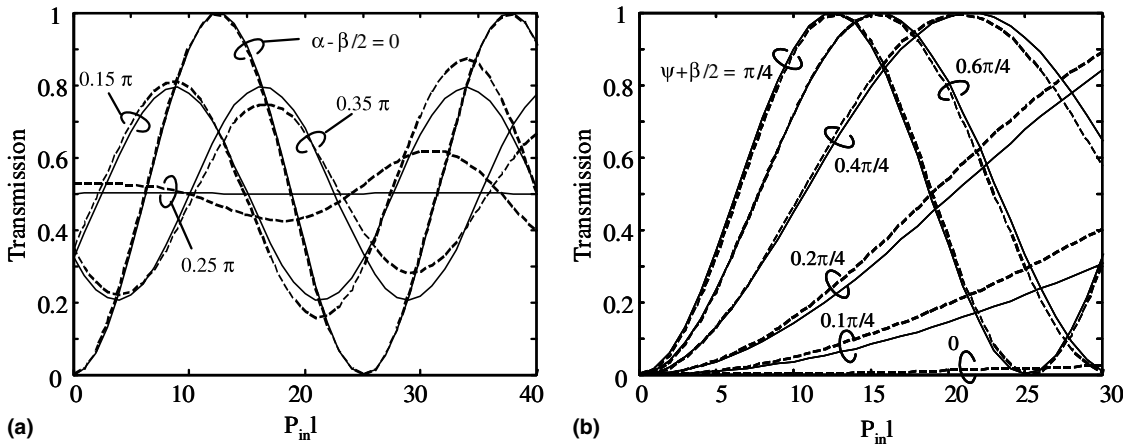

Fig. 2. NOLM transmission for (a) circular right and (b) linear input polarisations, for different values of the control parameter (α and ψ, respectively). In Fig. (b), $\alpha = \beta/2$. Solid lines: Eq. (10); dashed lines: curves obtained by integrating general nonlinear equations using $g = 100$ and $l = 10$.

power is a very attractive feature for several applications. However, adjusting α modifies not only P_π, but also the contrast, as well as the low-power transmission, so that an adjustment of P_π through the polarisation orientation ψ looks more convenient. For example, let us first set α in order to fix the contrast (e.g., for $\alpha = \beta/2$, contrast is infinite). Then, adjusting ψ allows to select for the critical power any value between $P_\pi = 4\pi/l$ and $P_\pi = \infty$, without change of contrast. The minimal value $P_\pi = 4\pi/l$ is obtained when $\psi = -\alpha + (2k + 1)\pi/4$, k integer, i.e., when the input polarisation makes an angle of 45° with the QWP axes (see Fig. 1), so that the CCW beam becomes circularly polarised ($A_s^{ccw} = \pm 1$). This situation is similar to Section 3.1, as in both cases the counterpropagating beams are polarised circularly and linearly, and the transmission takes the same expression as Eq. (12). The other extreme case, $P_\pi = \infty$, occurs when $\psi = -\alpha + k\pi/2$ (the input polarisation is aligned with one of the QWP axes). Both CW and CCW beams are then linearly polarised, no differential nonlinear effect appears and the transmission is constant versus P_{in}. Let us mention finally that the minimal critical value $P_\pi = 4\pi/l$ would be obtained, in a conventional NOLM having the same length, using a 0.58/0.42 coupling ratio. This value of P_π is thus relatively small.

Fig. 2(b) shows the transmission obtained using Eq. (13) for different values of ψ. Again, these results are compared with the curves obtained by numerical integration of the general coupled equations, taking $g = 100$ and $l = 10$. The agreement is seen to be good, some discrepancies appearing as a consequence of the low value of twist that was chosen.

It has to be noted finally that low-power transmission is independent on the input polarisation state, so that adjusting ψ does not modify the low-power value of the transmission (see Eq. (13) when $P_{in} = 0$). In particular, if $\alpha = \beta/2$, $T = 0$ for $P_{in} = 0$, independently on the polarisation orientation. The device thus looks very attractive for pulse reshaping applications. Indeed, the transmission characteristic can be easily optimised for both pedestal suppression and amplitude regularisation of an optical pulse train at a given power, through successive adjustments of the angles α and ψ.

3.3. Elliptic input polarisation

In the general case of elliptic input polarisation, and supposing that the ellipse axes are not aligned with the QWP axes, none of the two Stokes parameters A_s^{cw} and A_s^{ccw} is equal to zero. In this case, according to Eq. (10), the nonlinear term of the transmission is the product of two cosines, each of which is driven by one

of the Stokes parameters. Different input polarisations thus give rise to different behaviours of the transmission curve. Let us first consider that the Stokes parameters have very different magnitudes (one is close to zero, and the other close to ±1). This case is particularly interesting in practice, as it corresponds to the situation where the input polarisation is slightly elliptical (i.e., showing up a small deviation with respect to either purely circular or linear input polarisation states). In practice, even if exact circular or linear input polarisation is desired, in order to obtain one of the optimal transmission characteristics described in Sections 3.1 and 3.2, such a deviation is likely to exist, due to the imprecision of the adjustment procedure and possible drifts with time. Hence, it is important to analyse the impact of this deviation on the NOLM transmission.

This impact is illustrated in Fig. 3 in the case of a nearly linear polarisation making an angle of 45° with the QWP axes ($\alpha + \psi = \pi/4$). Because $A_s^{cw} \ll A_s^{ccw}$, the corresponding cosine functions oscillate at different speeds, the slower modulating the amplitude of the faster. In contrast, for exact linear input polarisation, no such modulation appears. In practice, the transmission characteristic is used up to one, or a few times the critical power only, and over this limited power range the slow modulation appears as a damping of the transmission characteristic, the maxima decreasing and the minima increasing (i.e., the contrast decreasing) with increasing input power. The situation is similar for nearly circular input polarisation. The damping of the transmission curve which was observed experimentally [14] could thus be easily related to an imperfect adjustment of input polarisation (although alternative explanations exist, like nonlinear spectral broadening). In most cases however, this effect is not likely to impose severe practical limitations. Indeed, an important parameter is the contrast between the first maxima and minima of the transmission curve. As low-power transmission does not depend on input polarisation state, the first minimum remains equal to zero even if the input polarisation suffers a deviation from linear or circular, and consequently contrast remains infinite.

A negative consequence however of an imperfect adjustment of input polarisation is a reduction of the first maximum of transmission. Fig. 4(a) shows the evolution of this first maximum in function of the input Stokes parameter, A_s^{cw}. Let us consider again the case of $\alpha + \psi = \pi/4$ (curve in bold). Starting from $A_s^{cw} = 0$ (linear input polarisation), the value of maximal transmission remains close to 1 for rather large excursions of the Stokes parameter, whereas it decreases sharply when A_s^{cw} deviates from ±1 (circular polarisation). To give an idea, maximum transmission remains higher than 0.9 for A_s^{cw} included between −0.2 and +0.2, whereas starting from $A_s^{cw} = \pm 1$, an excursion as small as 0.02 is sufficient to cause the transmission to drop to 0.9. Hence, some imprecision in the adjustment of linear input polarisation generates only limited loss, while in the case of circular polarisation, a substantial loss is to be expected, although never higher than

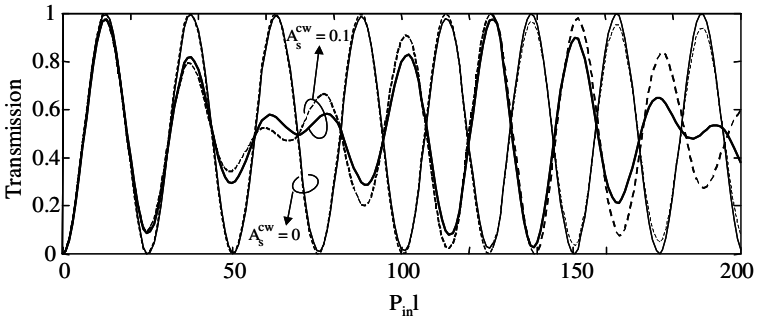

Fig. 3. NOLM transmission for exact linear ($A_s^{cw} = 0$) and slightly elliptic ($A_s^{cw} = 0.1$) input polarisations, when $\alpha = \beta/2$ and $\alpha + \psi = \pi/4$. Solid lines: Eq. (10); dashed lines: results obtained using general nonlinear equations for $g = 100$ and $l = 10$. Again, the correspondence between solid and dashed curves is shown to be good, small differences arising essentially from the infinite twist approximation.

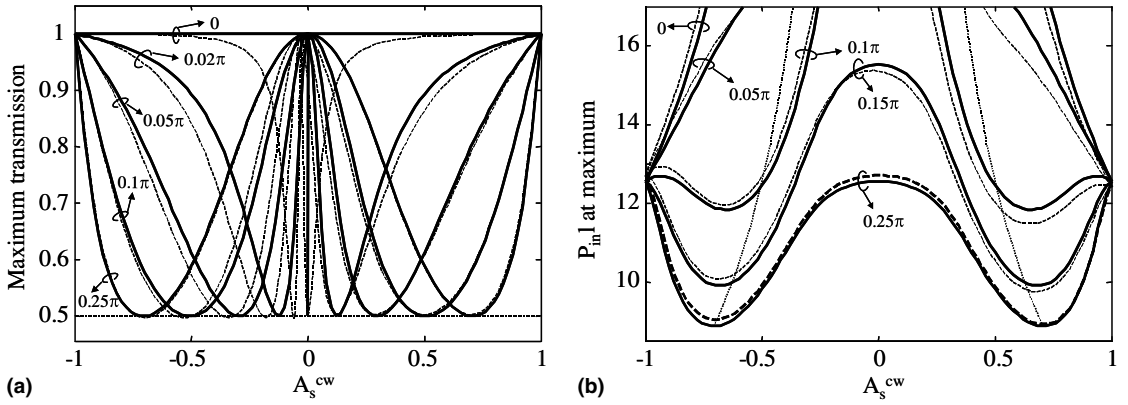

Fig. 4. Curves of transmission (a) and input power (b) at the first maximum of transmission when $\alpha = \beta/2$, as a function of input polarisation state. Values of $\alpha + \psi$ are given as curve labels. Solid lines: Eq. (10); dashed lines: results obtained by resolving general nonlinear equations for $g = 100$ and $l = 10$. Dotted curves: points for which $|A_s^{ccw}| = |A_s^{cw}|$.

50%. Note finally that the reduction of maximal transmission is accompanied by a reduction of the power at which this maximum occurs (Fig. 4(b)). It is convenient for the following to call this power the critical power (although in general it does not correspond to a π NPR difference).

In the discussion above, we considered the effect of a change of ellipticity, while the angle between the ellipse major axis and the QWP axes, $\alpha + \psi$, was π/4. A change of the ellipse orientation ψ (thus of $\alpha + \psi$) is also likely to take place in practice, and it is then important to consider the effects of such a deviation on the transmission characteristic. The curves of Fig. 4 were obtained for different values of $\alpha + \psi$, varied between 0 and π/4. For $A_s^{cw} = 0$, we are in the case we already tackled in Section 3.2. Fig. 4(a) shows that the maximum remains equal to 1 whatever the value of $\alpha + \psi$, although it is clear from Fig. 4(b) that, when $\alpha + \psi$ deviates from π/4, the critical power increases. This increase is slow however starting from $\alpha + \psi = \pi/4$. For example, it remains limited to about 10% for excursions as large as ±0.21 rad (±12°) of the angle ψ (this can be verified using the expression of critical power when $A_s^{cw} = 0, P_\pi = 4\pi/|l \sin 2(\alpha + \psi)|$). This observation remains valid if A_s^{cw} slightly differs from 0. In contrast, when $\alpha + \psi$ approaches 0, the critical power increases very fast and, for $\alpha + \psi = 0 + k\pi/2$, its value reaches infinity (see Section 3.2).

Let us now turn to the case of circular initial polarisation, $A_s^{cw} = \pm 1$. The transmission maximum is then equal to 1, and occurs at the same power whatever the value of ψ. This was of course expected, as circular polarisation has no preferential orientation. This conclusion has to be revised, however, when the Stokes parameter is slightly different from ±1. As already mentioned above, if $\alpha + \psi = \pi/4$, both transmission and power diminish abruptly after a small deviation of the Stokes parameter. This high sensitivity of transmission to input ellipticity remains over a rather wide domain of the parameter ψ centred on $-\alpha + \pi/4$. In contrast, when $\alpha + \psi$ gets close to 0, Fig. 4(a) shows that the maximal transmission is only little affected by a small deviation of A_s^{cw} from ±1. Fig. 4(b) shows however that such a deviation also leads to a rapid increase of the critical power.

In summary, once the QWP angle α has been adjusted for minimal low-power transmission, an optimal switching characteristic (with unity peak transmission occurring at reasonably low power) can be obtained if the input polarisation is set either circular, or linear making an angle of π/4 with respect to the QWP axes. The latter case in particular is interesting, as it makes the switching characteristic robust against possible fluctuations of the input polarisation (ellipticity and direction).

In Fig. 4, the curves obtained using the numerical approach to determine transmission characteristics are in general in good agreement with the curves obtained using Eq. (10). One exception however has to be mentioned, for $\alpha + \psi = 0$, when A_s^{cw} approaches 0 (see Fig. 4(a)) This case has little practical relevance

however, as the critical power is then very high. In spite of the high powers involved, the discrepancy was shown to originate from finite twist, and not from the low-power approximation.

From Fig. 4(b), it appears that the critical power is not minimal for purely linear or circular input polarisations. In fact, considering the curve $\alpha + \psi = \pi/4$, the critical power is even maximal for $A_s^{cw} = 0$ and $A_s^{cw} = \pm 1$. Its minimum over all values of A_s^{cw} and ψ is reached for two different input polarisation states, defined by $A_s^{cw} = \pm\sqrt{2}/2$ and $\psi = -\alpha + \pi/4(+k\pi/2)$. Although the lowest maximal transmission $T_{max} = 0.5$ is obtained for these values (Fig. 4(a)), this substantial reduction of critical power in comparison with the cases $A_s^{cw} = 0$ and $A_s^{cw} = \pm 1$ (by a factor of $\sqrt{2}$) is noticeable. For $A_s^{cw} = +\sqrt{2}/2$ and $\psi = -\alpha + \pi/4 + k\pi$ [for $A_s^{cw} = -\sqrt{2}/2$ and $\psi = -\alpha + \pi/4 + (2k + 1)\pi/2$], minimal critical power can be easily explained by noting [with the help of Eq. (11)] that $|A_s^{cw} - A_s^{ccw}|$ is maximal in this case, reaching $\sqrt{2}$ (for comparison, $|A_s^{cw} - A_s^{ccw}| = 1$ if the input polarisation is circular or linear at 45° from the QWP axes). The counterpropagating beams then have the same ellipticity, but opposite signs ($A_s^{cw} = -A_s^{ccw}$). As $|A_s^{cw} - A_s^{ccw}|$ is maximal, the difference between the nonlinear rotations undergone by the two ellipses is maximal, and the critical power minimal. Using Eq. (9), the transmission can be written as

$$T = \frac{1}{2} - \frac{1}{4}\cos 2(\beta - 2\alpha) - \frac{1}{4}\cos\left(\frac{\sqrt{2}}{4}P_{in}l\right). \tag{14}$$

The transmission is thus a sinusoidal function of power, whose amplitude is 1/2 and its critical power $P_\pi = 2\sqrt{2}\pi/l$, i.e., $\sqrt{2}$ times lower than in case 3.1 or than in case 3.2 when $\alpha + \psi = \pi/4$.

Let us now consider the other minimum in Fig. 4(b), observed for $A_s^{cw} = -\sqrt{2}/2$ and $\psi = -\alpha + \pi/4 + k\pi$ [or for $A_s^{cw} = +\sqrt{2}/2$ and $\psi = -\alpha + \pi/4 + (2k + 1)\pi/2$]. In this case, Eq. (11) shows that $A_s^{ccw} = A_s^{cw}$, which means that the counterpropagating beams have the same polarisation. Consequently, both ellipses undergo equal nonlinear rotations, so that their difference remains strictly equal to zero whatever the value of power. In other words, the effect of the fibre is identical on both beams ($F_{cw} = F_{ccw}$). In spite of this, a nonlinear transmission characteristic is still obtained, as shown by Eq. (15), which was derived using Eq. (9):

$$T = \frac{1}{4}\left[1 - \cos\left(2\beta - 4\alpha - \frac{\sqrt{2}}{4}P_{in}l\right)\right]. \tag{15}$$

This expression is very similar to Eq. (14), as transmission is again a sinusoidal function of power, with amplitude 1/2 and critical power $P_\pi = 2\sqrt{2}\pi/l$. The nonlinear behaviour observed here relies on the geometrical asymmetry of the loop. Indeed, the CW beam crosses successively the fibre span and the QWP, and a change in power modifies both the ellipticity and the ellipse orientation after the QWP (port 4). For the CCW, the order of these two elements is inverted, and a change in power results in a rotation of the ellipse at the end of the loop (port 3), but without change of ellipticity. Hence, at the NOLM output, because ellipticities and orientations of the two beams vary differently with power, the way they recombine (and thereby the transmission) is power-dependent. Formally, the non commutativity of the matrix product can be invoked to explain the existence of a nonlinear transmission in this case. Note however that, although transmission is power-dependent, the output polarisation state is not (see the following section).

Using Eq. (11), it appears that, for any value of the ellipse orientation ψ, there exist values of A_s^{cw} verifying the condition $|A_s^{ccw}| = |A_s^{cw}|$. For these input polarisation states, the transmission can be derived from Eq. (9), and is very similar to either Eqs. (14) or (15), except that the critical power is now given by $P_\pi = 2\pi/(A_s^{cw}l)$, which is higher than $2\sqrt{2}\pi/l$ ($|A_s^{ccw}| = |A_s^{cw}|$ implies that $|A_s^{cw}| \leqslant \sqrt{2}/2$). This dependence of P_π versus A_s^{cw} is shown in Fig. 4(b) as the dotted lines. We observe from the figure that, except in the case $\alpha + \psi = \pi/4$, the points of this curve do not match the minima of the curves at fixed ψ (the critical power is not minimal when $|A_s^{ccw}| = |A_s^{cw}|$, in general). In contrast, the peak transmission is always minimal, $T_{max} = 0.5$, when $|A_s^{ccw}| = |A_s^{cw}|$ (Fig. 4(a)).

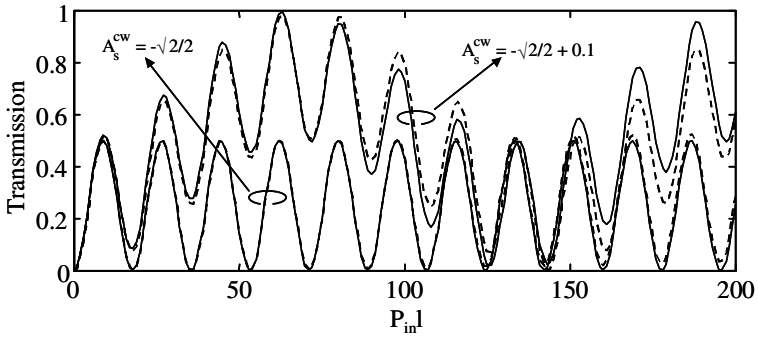

Fig. 5. NOLM transmission for $A_s^{cw} = -\sqrt{2}/2$ and $A_s^{cw} = -\sqrt{2}/2 + 0.1$, with $\alpha = \beta/2$ and $\alpha + \psi = \pi/4$ in both cases. Solid lines: Eq. (10); dashed lines: results obtained by resolving general nonlinear equations for $g = 100$ and $l = 10$. A good agreement is observed between the corresponding curves.

Fig. 4 shows that, for $|A_s^{cw}| = \sqrt{2}/2$ and $\alpha + \psi = \pi/4$, the switching characteristic is little affected by small changes in the ellipticity or direction of the input polarisation. If such small deviation takes place, both Stokes parameters are no longer strictly equal, although $\||A_s^{ccw}| - |A_s^{cw}\| \ll |A_s^{ccw}| + |A_s^{cw}|$. Eq. (9) shows that in this case, the transmission is the sum of two sinusoidal functions of power, oscillating at very different speeds. The result is depicted in Fig. 5, in the case of a small deviation of A_s^{cw} (a similar result is obtained for a small deviation of ψ). Although this deviation modifies drastically the transmission for high values of power, the changes are small for input powers ranging as P_π. In particular, the values of P_π and T_{max} (first maximum) are robust to these changes.

4. Conditions for power-independent output polarisation

In general, even if the polarisation at the NOLM input is fixed, the output polarisation is power-dependent, just like the transmission is. This may be a problem for polarisation-sensitive applications. Some cases exist however where a constant output polarisation is observed. It happens if the output Stokes parameter, $A_s^{out} = (|C_{out}^+|^2 - |C_{out}^-|^2)/(|C_{out}^+|^2 + |C_{out}^-|^2)$, as well as the output polarisation direction, ψ^{out}, are independent of power. Making use of Eqs. (7)–(9), one can show that power-independent output polarisation is obtained in the cases described below.

4.1. Circular (right or left) input polarisation

In this case, we find that A_s^{out} is constant versus power only if $\alpha = \beta/2 + k\pi/2$, k integer. Eq. (12) shows that, under such conditions, low-power transmission is minimal (=0) and maximal transmission is unity (infinite contrast). Output polarisation is then linear ($A_s^{out} = 0$). The value of ψ^{out} is constant with power and (unlike A_s^{out}) is also independent of α. Its value is given by $\psi^{out} = \beta/2 \pm \pi/4$. When $\alpha = \beta/2 + k\pi/2$, the upper sign holds if k is even for circular-right input, and if k is odd for circular-left input, the lower sign should be chosen otherwise. For other values of α, the sign depends on power, as the directions of the major and minor axes of the ellipse are periodically swapped due to changes of ellipticity that take place when power varies (see Fig. 6).

4.2. Linear input polarisation

In this case, we find again that A_s^{out} is power-independent only if $\alpha = \beta/2 + k\pi/2$, k integer. The Stokes parameter at the output is then given by $A_s^{out} = \mp \sin(\beta + 2\psi)$, the upper sign holding if k is

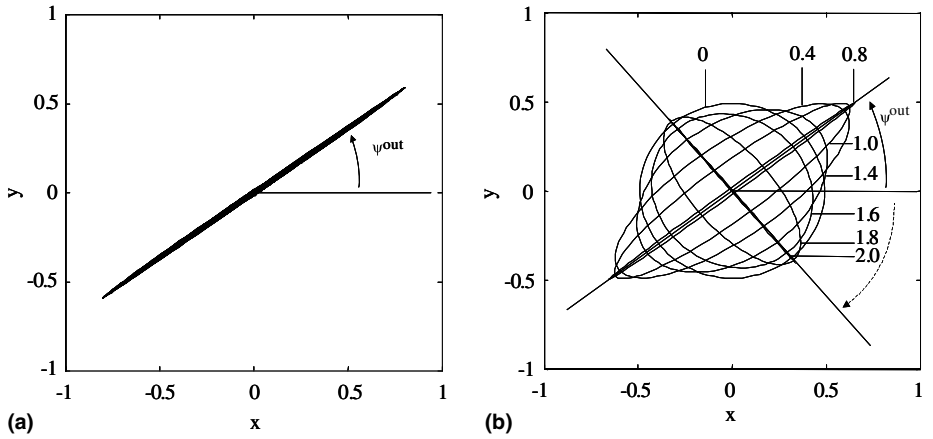

Fig. 6. Polarisation evolution at the NOLM output for growing input power P_{in} (given as curve labels), in the case of circular right input polarisation (x, y normalised to $\sqrt{P_{in}}$). We used $\alpha = \beta/2$ (a) and $\alpha = \beta/2 + 0.2\pi$ (b). Results were obtained by resolving general nonlinear equations for $g = 100$ and $l = 10$. See also Fig. 2(a).

even, and the lower if k is odd. Note that A_s^{out} is constant versus power whatever the value of ψ. However, even for $\alpha = \beta/2 + k\pi/2$, the output ellipse rotates with power. Its power-dependent direction is then given by:

$$\begin{aligned}\psi^{out} &= \frac{\beta}{2} \pm \frac{1}{8}\sin(2\psi+\beta)P_{in}l + \frac{\pi}{2}, \quad -\frac{\pi}{4} + m\pi < \psi + \frac{\beta}{2} < \frac{\pi}{4} + m\pi;\\ \psi^{out} &= \frac{\beta}{2} \pm \frac{1}{8}\sin(2\psi+\beta)P_{in}l, \quad \frac{\pi}{4} + m\pi < \psi + \frac{\beta}{2} < \frac{3\pi}{4} + m\pi,\end{aligned} \tag{16}$$

where m is an integer. Again, the upper signs are for k even, and the lower for k odd. Eq. (16) shows that ψ^{out} is independent of power only if $\psi = -\beta/2 + q\pi/2 = -\alpha + q\pi/2$, q integer. This case however (input polarisation aligned with one of the QWP axes) is not interesting in practice, as the NOLM transmission remains equal to zero for all values of power (see Section 3.2). A much more interesting situation appears for $\psi = -\beta/2 + (2m+1)\pi/4$. We find in this case that $A_s^{out} = \pm 1$, i.e., the output polarisation is circular. Although the rate of the ellipse rotation with power is maximal in this case, as shown by Eq. (16), it has no effect on the circular polarisation.

In summary, if the input polarisation is linear, power-independent output polarisation is obtained if $\alpha = \beta/2 + k\pi/2$, and the input polarisation making an angle of 45° with respect to the QWP axes. This situation corresponds to infinite contrast and minimal critical power (see Eq. (13)). The output polarisation in this case is depicted in Fig. 7(a). The slight ellipticity observed in the figure is due to the finite twist considered in calculations. Fig. 7(b) and (c) show the evolution of output polarisation for other orientations of the input polarisation with respect to the QWP.

4.3. Elliptic input polarisation

For general elliptic polarisation, the only possibilities to observe power-independent output polarisation are $A_s^{cw} = \pm A_s^{ccw}$ (see also Section 3.3).

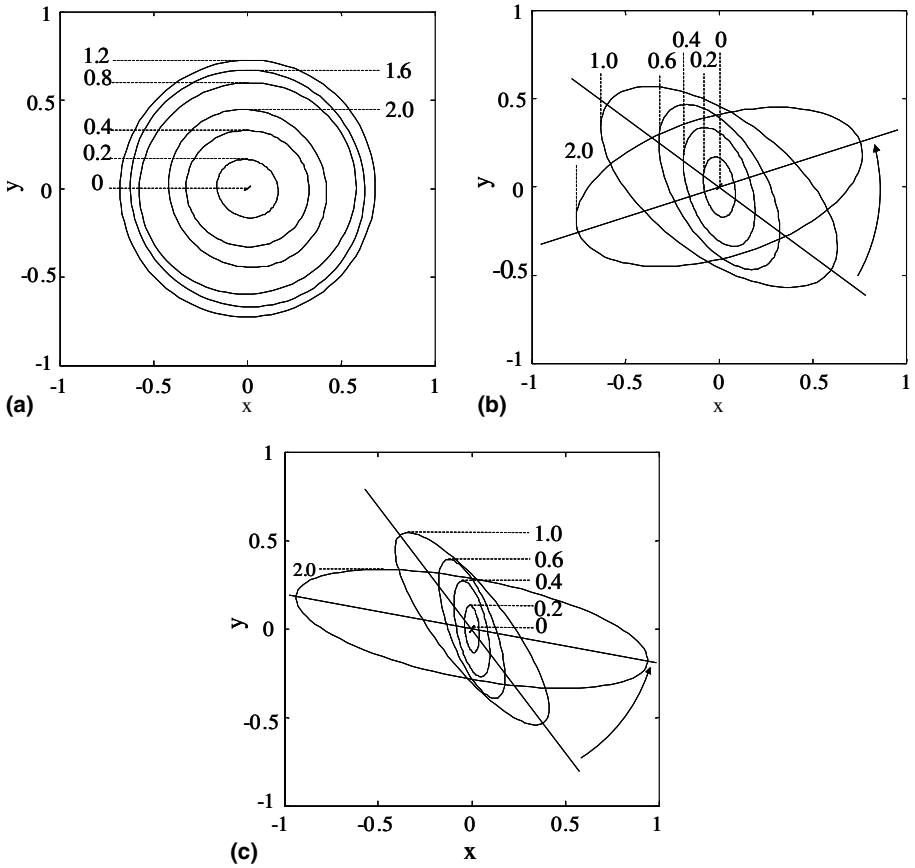

Fig. 7. Polarisation evolution at the NOLM output for growing input power P_{in} (given as curve labels), in the case of linear input polarisation (x, y normalised to $\sqrt{P_{in}}$). We used $\alpha + \psi = \pi/4$ (a), $0.6\pi/4$ (b) and $0.4\pi/4$ (c), and $\alpha = \beta/2$ in all cases. Arrows in (b) and (c) materialise the different rotations undergone by the ellipse for the same power increase (from $P_{in} = 1$ to 2). Results were obtained by resolving general nonlinear equations for $g = 100$ and $l = 10$. See also Fig. 2(b).

(a) $A_s^{cw} = A_s^{ccw}$.

In this case, the output polarisation is always found to be constant versus power. For any values of and ψ, there exists a value of A_s^{cw} obeying $A_s^{cw} = A_s^{ccw}$. Using Eq. (11), we find that this condition leads to

$$A_s^{cw} = \frac{-\sin 2(\alpha+\psi)}{\sqrt{1+\sin^2 2(\alpha+\psi)}}. \tag{17}$$

If this condition is fulfilled, the output polarisation is independent of power, and is given by $A_s^{out} = -A_s^{cw}$ and $\psi^{out} = -\psi + \pi/2$ (Fig. 8).

(b) $A_s^{cw} = -A_s^{ccw}$.

For given values of α and ψ, the input Stokes parameter is now given by

$$A_s^{cw} = \frac{\sin 2(\alpha+\psi)}{\sqrt{1+\sin^2 2(\alpha+\psi)}}. \tag{18}$$

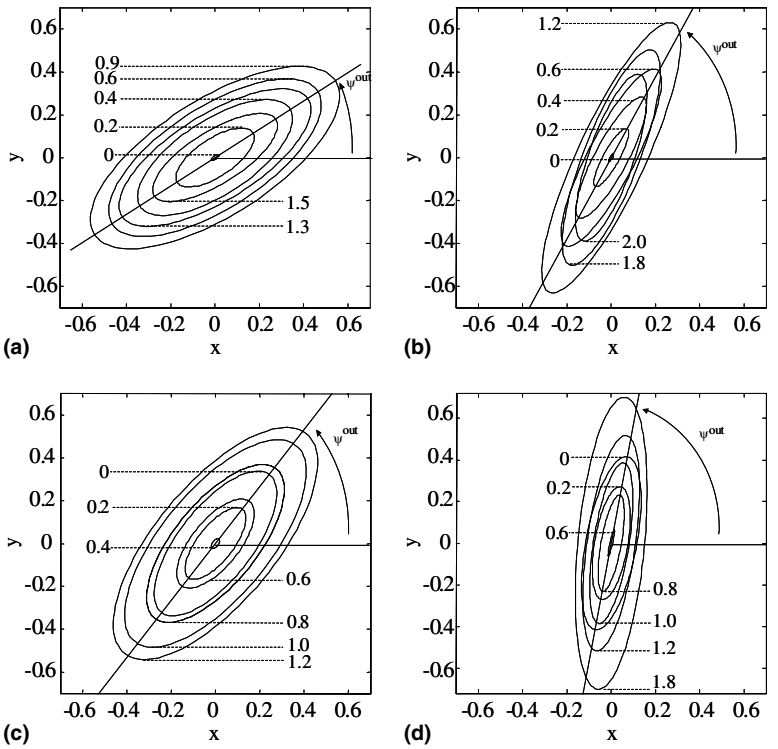

Fig. 8. Polarisation evolution at the NOLM output for growing input power P_{in} (given as curve labels) when $A_s^{cw} = A_s^{ccw}$ (x, y normalised to $\sqrt{P_{in}}$). The parameters are $\alpha = \beta/2$ (a,b) and $\alpha = \beta/2 + 0.4\pi/4$ (c,d), $\alpha + \psi = \pi/4$ (a,c) and $\alpha + \psi = 0.4\pi/4$ (b,d). Results were obtained by resolving general nonlinear equations for $g = 100$ and $l = 10$. The small variations of the ellipse direction observed in figures (b) and (d) are related to the finite value of twist.

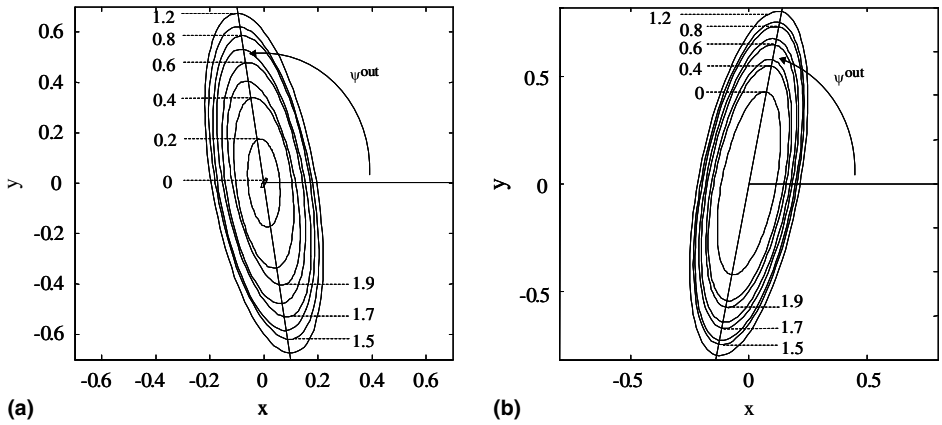

Fig. 9. Polarisation evolution at the NOLM output for growing input power P_{in} (given as curve labels) when $A_s^{cw} = -A_s^{ccw}$ (x, y normalised to $\sqrt{P_{in}}$). The parameters are $\alpha = \beta/2$ and $\psi = -\beta/2 + 0.1\pi$ (a), and $\alpha = \beta/2 + 0.1\pi$ and $\psi = -\beta/2$ (b). Results were obtained by resolving general nonlinear equations for $g = 100$ and $l = 10$. Again, small variations of the ellipse direction must be attributed to the finite value of twist.

In this case however, the output polarisation is not constant versus power, for general values of α and ψ. Power independence occurs only in two particular cases: either if $\alpha = \beta/2 + k\pi/2$, independently of ψ, or if $\psi = -\beta/2 + k\pi/2$, independently of α. In the first case, we find that $A_s^{out} = A_s^{cw}$ and $\psi^{out} = \beta + \psi + \pi/2$. In the second, $A_s^{out} = -A_s^{cw}$ and $\psi^{out} = \beta/2$ for k odd, or $\psi^{out} = \beta/2 + \pi/2$ for k even (Fig. 9).

5. Conclusion

In this paper, we analysed theoretically the operation of a novel NOLM scheme, whose switching is based on NPR. The device is composed of a symmetrical coupler, highly twisted fibre and a quarter wave plate inserted in the loop, close to one of the coupler output ports. Using a weak nonlinearity approximation, we showed that the NOLM operation can be advantageously described using a matrix approach. This analysis leads to a general analytical expression of the NOLM transmission, which is valid in the case of high twist. Thanks to this result, we showed that the NOLM transmission is extremely flexible. In particular, through adjustment of the QWP angle and of the input polarisation orientation and ellipticity, one can easily adjust the contrast or the critical power of the transmission characteristic over a wide range. This, together with some outstanding properties like the possibility to obtain infinite contrast, zero low-power transmission and unity peak transmission, makes the device very attractive for a wide spectrum of applications, including switching and pulse reshaping (amplitude regularisation, pedestal suppression). Using the model, we also showed that, for particular values of the control parameters, the transmission characteristic is stable against small variations of the input polarisation state, which are likely to occur in practice. This analysis also allowed us to determine the conditions under which output polarisation is power-independent, a situation that is particularly interesting in the frame of polarisation-sensitive applications. Quite interestingly, we showed that, even in the case where the system is symmetric in both power and polarisation (i.e., when neither nonlinear phase shift difference, nor NPR difference exist between the interacting beams), nonlinear switching can still occur, due to the geometrical asymmetry of the device. Our approach was shown to agree well with the results obtained using general coupled nonlinear equations in the continuous-wave case, even in the case of relatively low twist. As discussed elsewhere [11], we believe that such a continuous-wave analysis remains accurate for the description of practical systems where pulses down to a few*ps* in duration are used. We thus believe that the proposed analysis will provide a very useful tool to guide the application of the proposed architecture in future ultrafast optical systems.

Acknowledgements

This work was supported by F.N.R.S. (Belgian Fund for Scientific Research), by the Interuniversity Attraction Pole IAP V/18 program of the Belgian Science Policy, and by CONACyT (Mexican Council for Science and Technology). This work was also funded by CONACyT Project J36135-A.

References

[1] N.J. Doran, D. Wood, Opt. Lett. 13 (1988) 56.
[2] H. Sotobayashi, C. Sawaguchi, Y. Koyamada, W. Chujo, Opt. Lett. 27 (2002) 1555.
[3] W.W. Tang, C. Shu, K.L. Lee, IEEE Photon. Technol. Lett. 13 (2001) 16.
[4] I.N. Duling III, Opt. Lett. 16 (1991) 539.
[5] M.D. Pelusi, Y. Matsui, A. Suzuki, IEEE J. Quantum Electron. 35 (1999) 867.

[6] A. Bogoni, P. Ghelfi, M. Scaffardi, L. Potì, IEEE J. Select. Top. Quantum Electron. 10 (2004) 192.
[7] H.Y. Rhy, B.Y. Kim, H.-W. Lee, Opt. Commun. 147 (1998) 47.
[8] E.A. Kuzin, N. Korneev, J.W. Haus, B. Ibarra-Escamilla, J. Opt. Soc. Am. B 18 (2001) 919.
[9] O. Pottiez, E.A. Kuzin, B. Ibarra-Escamilla, F. Méndez Martínez, Opt. Commun. 229 (2004) 147.
[10] S.F. Feldman, D.A. Weinberger, H.G. Winful, J. Opt. Soc. Am. B 10 (1993) 1191.
[11] O. Pottiez, E.A. Kuzin, B. Ibarra-Escamilla, J.T. Camas-Anzueto, F. Gutiérrez-Zainos, Opt. Express 17 (2004) 3878.
[12] O. Pottiez, E.A. Kuzin, B. Ibarra-Escamilla, F. Gutiérrez-Zainos, U. Ruiz-Corona, J.T. Camas-Anzueto, IEEE Photon. Technol. Lett. 17 (2005) 154.
[13] E.A. Kuzin, B. Ibarra Escamilla, D.E. Garcia-Gomez, J.W. Haus, Opt. Lett. 26 (2001) 1134.
[14] O. Pottiez, E.A. Kuzin, B. Ibarra-Escamilla, J.T. Camas-Anzueto, F. Gutiérrez-Zainos, Electron. Lett. 40 (2004) 892.